Orientation Effects in 2–2 Composites Based on [011]-poled PZN–0.065PT Single Crystal

V. Yu. Topolov[1](✉), A. N. Isaeva[1], and A. V. Krivoruchko[2]

[1] Department of Physics, Southern Federal University, Rostov-On-Don, Russia
vutopolov@sfedu.ru
[2] Don State Technical University, Rostov-On-Don, Russia

Abstract. Results on orientation dependences of effective piezoelectric coefficients d_{3j}^*, electromechanical coupling factors k_{3j}^*, traditional energy-harvesting figures of merit $d_{3j}^* g_{3j}^*$ and modified energy-harvesting figures of merit $F_{3j}^{*\sigma}$ are reported for 2–2 composites based on [011]-poled domain-engineered $0.935Pb(Zn_{1/3}Nb_{2/3})O_3$–$0.065PbTiO_3$ single crystal with high piezoelectric activity. A rotation of the main X and Y crystallographic axes around the Z-axis in each crystal layer of the composites is considered, and the volume fraction of the single-crystal component m varies from 0.1 to 0.5. An analogy between the orientation dependences of d_{3j}^* and k_{3j}^* as well as between $d_{3j}^* g_{3j}^*$ and $F_{3j}^{*\sigma}$ is shown at $m = \text{const}$. Maxima of the longitudinal parameters d_{33}^*, $d_{33}^* g_{33}^*$ and $F_{33}^{*\sigma}$ at $m = \text{const}$ are observed in a relatively narrow orientation range. Due to large values of the studied parameters, the 2–2 composites are of interest as active elements of piezoelectric transducers, sensors and energy-harvesting systems.

Keywords: 2–2 composite · Piezoelectric coefficient · Rotation angle · Crystallographic axes · Orientation dependence

1 Introduction

Piezo-active 2–2 composites based on domain-engineered single crystals (SCs) are advanced dielectric materials with large piezoelectric coefficients, electromechanical coupling factors (ECFs), figures of merit (FOMs), hydrostatic and other important parameters [1–4]. Orientation effects in these composites [1, 3, 4] are mainly concerned with rotations of crystallographic axes in the SC component. The SC component is often chosen among high-performance relaxor-ferroelectrics, for instance, $(1-x)Pb(Zn_{1/3}Nb_{2/3})O_3-xPbTiO_3$ (PZN–xPT) [5–7] or $(1-x)Pb(Mg_{1/3}Nb_{2/3})O_3$–$xPbTiO_3$ (PMN–xPT) with perovskite-type structures and compositions near the morphotropic phase boundary. SC samples are poled along one of the following unit-cell directions [3, 5–7]: [001], [011] or [111]. The poled SC samples are domain-engineered, with non-180° domain types therein. The aforementioned rotations of the crystallographic axes are taken into account when predicting the effective electromechanical properties and related parameters of the 2–2 composites [1, 3, 4]. In the present chapter, we show an effect of the rotation of the main crystallographic axes in the [011]-poled SC

I. A. Parinov et al. (Eds.): *Physics and Mechanics of New Materials and Their Applications*, SPM 20, pp. 93–103, 2023. https://doi.org/10.1007/978-3-031-21572-8_9

component on the piezoelectric performance, ECFs and energy-harvesting FOMs of the parallel-connected 2–2 relaxor-ferroelectric SC / polymer composites. Hereby the piezoelectric component is the [011]-poled domain-engineered PZN– 0.065PT SC with a high piezoelectric activity [7] and full set of experimental electromechanical constants (Table 1).

Table 1 Elastic compliances s^E_{ab} (in 10^{-12} Pa^{-1}), piezoelectric coefficients d_{ij} (in pC/N) and dielectric permittivities $\varepsilon^{\sigma}_{pp}$ of [011]-poled domain-engineered PZN–0.065PT SC (macroscopic *mm*2 symmetry) and polyethylene (isotropic material) at room temperature

Electromechanical constants	PZN–0.065PT [7]	Polyethylene [3]
s^E_{11}	46.99	1540
s^E_{12}	−74.01	−517
s^E_{13}	39.51	−517
s^E_{22}	170.69	1540
s^E_{23}	−96.76	−517
s^E_{33}	61.47	1540
s^E_{44}	15.04	4114
s^E_{55}	333.33	4114
s^E_{66}	169.08	4114
d_{15}	4871	0
d_{24}	121	0
d_{31}	1191	0
d_{32}	– 2618	0
d_{33}	1571	0
$\varepsilon^{\sigma}_{11}/\varepsilon_0$	9500	2.3
$\varepsilon^{\sigma}_{22}/\varepsilon_0$	1500	2.3
$\varepsilon^{\sigma}_{33}/\varepsilon_0$	5600	2.3

2 Model Concepts, Effective Electromechanical Properties and Parameters of the 2–2 Composite

2.1 Model of the 2–2 Composite

The 2–2 composite is characterised as a system of parallel-connected layers of two types, and these layers are regularly arranged along the OX_1 axis (Fig. 1). The interfaces that separate the SC and polymer layers are parallel to the (X_2OX_3) plane. In our model, a

Type I layer represents a domain-engineered SC with a spontaneous polarisation $\boldsymbol{P_s}^{(1)}$, see inset 1 in Fig. 1. The *Type II* layer is polymer medium (inset 2 in Fig. 1). In the initial position, the main crystallographic axes X, Y and Z in each SC layer (Type I) are oriented as follows: $X \parallel OX_1$, $Y \parallel OX_2$ and $Z \parallel \boldsymbol{P_s}^{(1)} \parallel OX_3$. The main crystallographic axes in each SC layer are expressed in terms of the perovskite unit-cell direction [h k l] in the following form: $X \parallel [0\ \bar{1}\ 1]$, $Y \parallel [1\ 0\ 0]$ and $Z \parallel [011]$. A rotation of the main crystallographic axes X, Y around the main crystallographic Z-axis is performed in the (X_1OX_2) plane, and the rotation angle φ is shown in the inset 1 in Fig. 1. At this rotation mode, a poling Z-axis is parallel to the co-ordinate OX_3 axis for both the Type I layer and composite at any φ values [1, 4].

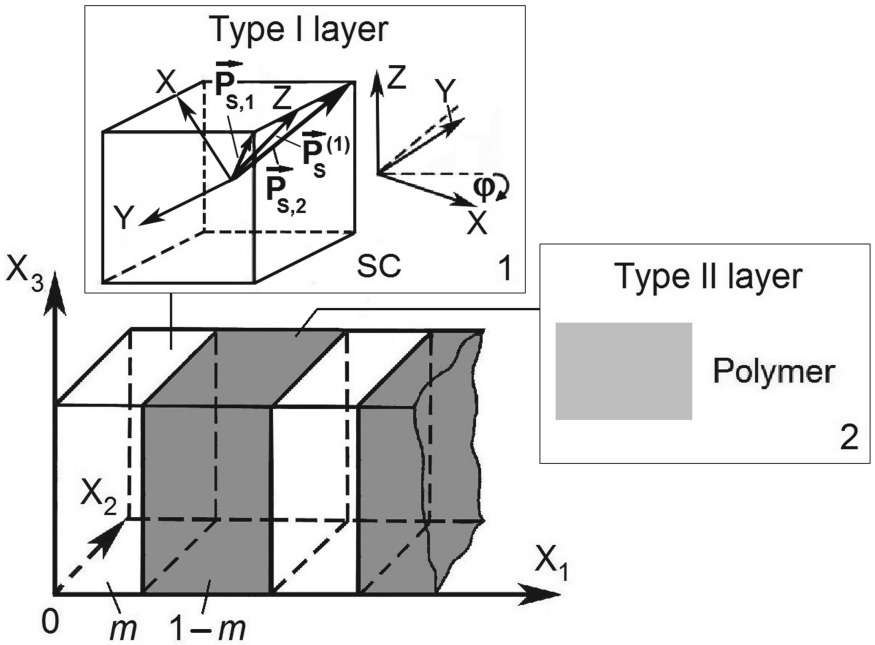

Fig. 1 Schematic of the 2–2 SC /polymer composite; $(X_1X_2X_3)$ is the rectangular co-ordinate system; m and $1 - m$ are volume fractions of the Type I (domain-engineered SC, inset 1) and Type II (polymer, inset 2) layers, respectively. In inset 1, orientations of domains with spontaneous polarisations $\boldsymbol{P_{s,j}}$ and mode of the rotation of the main crystallographic axes X and Y in the SC component are shown, where φ is the rotation angle (reprinted from paper by Topolov [4], with permission from the Royal Society of Chemistry)

2.2 Effective Electromechanical Properties and Parameters at the Rotation of Main Crystallographic Axes

Averaging the electromechanical properties along the OX_1 axis is performed in terms of the matrix method by taking into consideration boundary conditions [3, 4] for electric

and mechanical fields in the adjacent layers of the parallel-connected 2–2 composite (Fig. 1).

These boundary conditions at the interface $x_1 = \text{const}$ involve the continuity of the following components:

(i) three normal components of the mechanical stress (σ_{11}, σ_{12} and σ_{13}),
(ii) three tangential components of the mechanical strain (ξ_{22}, ξ_{23} and ξ_{33}),
(iii) one normal component of the electric displacement (D_1),
(iv) two tangential components of the electric field (E_2 and E_3).

The effective electromechanical properties of the 2–2 composite are described by the matrix [3]:

$$\left|\left|C^*\right|\right| = \left[\left|\left|C^{(1)}\right|\right| \cdot ||M||m + \left|\left|C^{(2)}\right|\right| (1-m)\right][||M||m + ||I||(1-m)]^{-1}, \quad (1)$$

where $\| C^{(n)} \| = \begin{pmatrix} \| s^{(n),E} \| & \| d^{(n)} \|^T \\ \| d^{(n)} \| & \| \varepsilon^{(n),\sigma} \| \end{pmatrix}$ (9 × 9 matrix) charcterises the properties of SC ($n = 1$) or polymer ($n = 2$), and superscript 'T' denotes the transposed matrix. In Eq. (1), $\| M \|$ is the 9 × 9 matrix concerned with the aforementioned boundary conditions at $x_1 = \text{const}$, $\| I \|$ is the 9 × 9 identity matrix, and m is the volume fraction of the SC component. The $\| C^* \|$ matrix from Eq. (1) is the 9 × 9 matrix that is represented as

$$\left|\left|C^*\right|\right| = \begin{pmatrix} \| s^{*E} \| & ||d^*||^t \\ ||d^*|| & ||\varepsilon^{*\sigma}|| \end{pmatrix}. \quad (2)$$

In Eq. (2), $\| s^{*E} \|$ is the 6 × 6 matrix of elastic compliances at $E = \text{const}$, $\| d^* \|$ is the 6 × 3 matrix of piezoelectric coefficients, and $\| \varepsilon^{*\sigma} \|$ is the 3 × 3 matrix of dielectric permittivities at $\sigma = \text{const}$. Elements of the $\| C^{(1)} \|$ matrix are found by taking into account the main crystallographic axes X, Y around Z in each SC layer, and its electromechanical constants are written as tensor components:

$$\varepsilon^{\sigma'}_{mn} = r_{mp} r_{nq} \varepsilon^{\sigma}_{pq},\ d'_{efg} = r_{ej} r_{fk} r_{gl} d_{jkl} \text{ and } S^{E'}_{rtuv} = r_{ra} r_{tb} r_{uc} r_{vd}\, S^{E}_{abcd}. \quad (3)$$

In Eqs. (3), r_{mp} is the element of the rotation matrix $\| r \|$ that depends on the rotation angle φ. In right parts of Eqs. (3), $\varepsilon^{\sigma}_{pq}$, d_{jkl} and s^{E}_{abcd} are tensor components of dielectric permittivities (second rank), piezoelectric coefficients (third rank) and elastic compliances (fourth rank), respectively. The electromechanical constants from Eqs. (3) are to be written in the two-index (or matrix) form [3] and included in the $\| \varepsilon^{(1),\sigma} \|$, $\| d^{(1)} \|$ and $\| s^{(1),E} \|$ matrices that are parts of the $\| C^{(1)} \|$ matrix from Eq. (1).

The 2–2 composite (Fig. 1) can be characterised by the full set of s^{*E}_{ab}, d^*_{ij} and $\varepsilon^{*\sigma}_{fh}$ from $\| C^* \|$ in Eq. (1), and the $\| C^* \|$ matrix depends on the volume fraction m and rotation angle φ. The effective electromechanical properties of the composite are found in the longwave approximation [3, 4], when the wavelength of the external acoustic field is much greater than the width of each layer of the composite sample. Based on the $\| C^* \|$ matrix from Eq. (1), we analyse the orientation effect and following effective parameters of the 2–2 composite:

(i) piezoelectric coefficients $d_{3j}{}^{*}$,
(ii) ECFs

$$k_{3j}^{*} = d_{3j}^{*} / (s_{jj}^{*E})^{1/2}, \tag{4}$$

(iii) traditional (or squared) energy-harvesting FOMs

$$\left(Q_{3j}^{*}\right)^{2} = d_{3j}^{*} g_{3j}^{*}, \tag{5}$$

(iv) modified FOMs [8, 9] for a stress-driven system

$$F_{3j}^{*\sigma} = L_{3j}^{*}\left(Q_{3j}^{*}\right)^{2}, \tag{6}$$

where $j = 1, 2$ and 3. The piezoelectric coefficients $d_{3j}{}^{*}$ and $g_{3j}{}^{*}$ from Eq. (5) are related [10] as follows:

$$d_{3j}^{*} = \varepsilon_{3f}^{*\sigma} g_{fj}^{*} \tag{7}$$

In Eq. (6),

$$L_{3j}^{*} = [(k_{3j}^{*})^{-1} - ((k_{3j}^{*})^{-2} - 1)^{1/2}]^{2} / (k_{3j}^{*})^{2} \tag{8}$$

is the 'maximum output electrical energy/stored electrical energy' ratio [8] that depends on ECFs $k_{3j}{}^{*}$ from Eq. (4). It should be noted that ECFs $k_{3j}{}^{*}$ from Eq. (4) are taken as absolute values in accordance with work [8, 9]. ECFs $k_{3j}{}^{*}$ from Eq. (4), FOMs $(Q_{3j}{}^{*})^{2}$ from Eq. (5) and $F_{3j}{}^{*\sigma}$ from Eq. (6) are of importance to evaluate an effectiveness of a piezoelectric material from a viewpoint of energy conversion [8–10].

To evaluate the effective electromechanical properties and related parameters (4)–(6) of the 2–2 composite, we use experimental data (Table 1) on the [0 1 1]-poled PZN–0.065PT SC and polyethylene. The PZN–0.065PT SC is of interest as a piezoelectric component that promotes high piezoelectric activity and sensitivity of the related 2–2-type composites highlighted recently [4]. It should be added that the PZN–0.065PT SC is characterised by the large value of $|d_{32}|$ in comparison to d_{31} and d_{33}, see Table 1. The $|d_{32}|$ value from Table 1 is comparable to the d_{33} value of the [0 0 1]-poled PZN–xPT and PMN–xPT SCs, see, for example data in Refs. [3] and [12].

3 Orientation Dependences of Effective Piezoelectric Properties and Related Parameters

Examples of the orientation (φ) dependences of the effective piezoelectric coefficients $d_{3j}{}^{*}$ of the parallel-connected 2–2 composite are shown in Fig. 2. It is sufficient to consider these orientation dependences in the range of $0° \leq \varphi \leq 90°$ because the effective electromechanical properties of the composite Φ^{*} obey the condition $\Phi^{*}(m, \varphi) = \Phi^{*}(m, 180° - \varphi)$. We remind the reader that the main piezoelectric component is the [011]-poled PZN–0.065PT SC with macroscopic $mm2$ symmetry [7]. We assume that the volume fraction of the SC component is $m = \text{const}$, and we consider some m

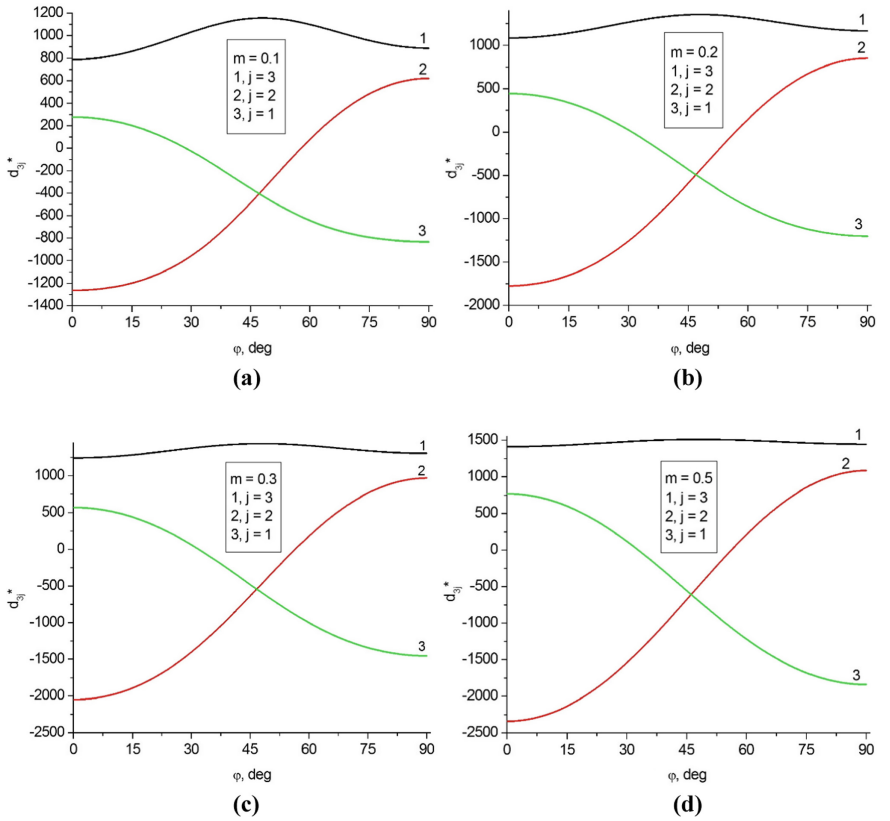

Fig. 2 Orientation dependences of piezoelectric coefficients d_{3j}^* (in pC / N) of the 2–2 PZN–0.065PT SC /polyethylene composite at volume fractions of SC $m = 0.1$ (a), $m = 0.2$ (b), $m = 0.3$ (c), and $m = 0.5$ (d)

values from 0.1 to 0.5. In general, increasing the volume fraction m leads to a higher piezoelectric activity of the 2–2 composite. For instance, in the vicinity of the diffuse maximum, the longitudinal piezoelectric coefficient d_{33}^* (curve 1 in Fig. 2) increases by about 1.4 times when increasing the volume fraction m from 0.1 to 0.5. At the rotation angle $\varphi = 45°$, irrespective of the volume fraction m, the equality of the piezoelectric coefficients $d_{3|}^* = d_{32}^*$ holds, see curves 2 and 3 in Fig. 2.

Comparing graphs from Fig. 3 to graphs from Fig. 2 at the volume fraction $m =$ const, we note a similar character of the orientation dependences of the piezoelectric coefficients d_{3j}^* and ECFs $k_{3j}^* \sim d_{3j}^*$, where $j = 1$, 2 and 3. However the equality of ECFs $k_{3|}^* = k_{32}^*$ holds at a rotation angle φ that differs from 45° (see Fig. 3), and this is accounted for by an influence of the dielectric and elastic properties on ECFs in accordance with Eq. (4). Graphs in Fig. 3 suggest that this influence undergoes minor changes on increasing the volume fraction m from 0.1 to 0.5.

One can draw an analogy between the orientation dependences of FOMs $(Q_{3j}^*)^2$ (Fig. 4) and $F_{3j}^{*\sigma}$ (Fig. 5) at $m =$ const. This analogy is due to a weak influence of

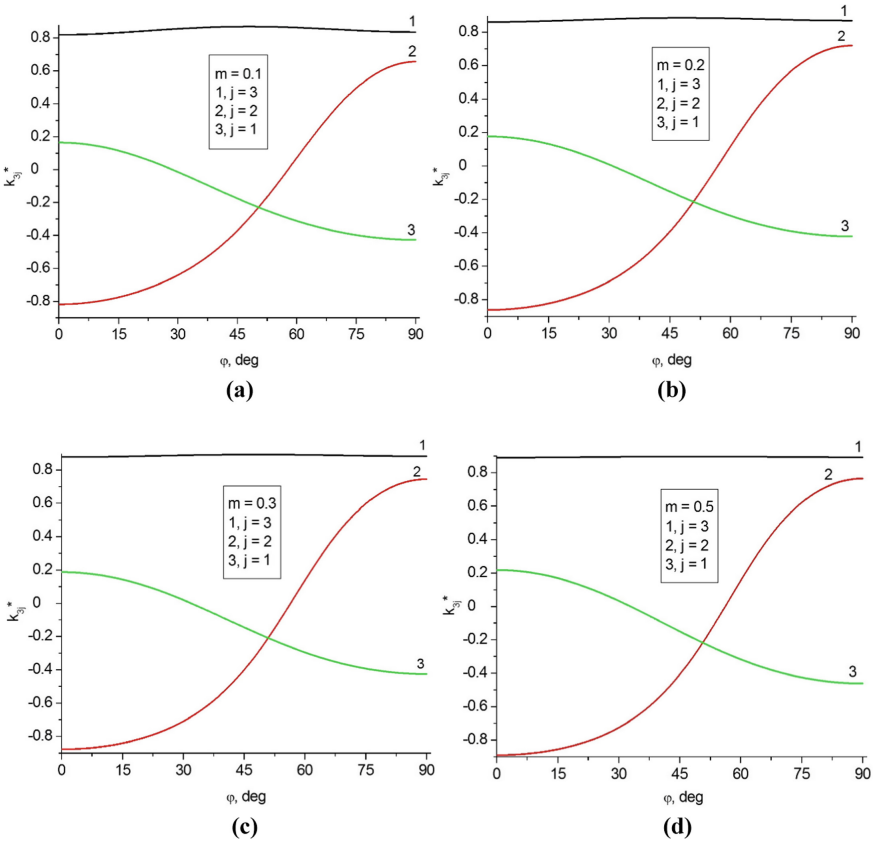

Fig. 3 Orientation dependences of ECFs $k_{3j}{}^{*}$ of the 2–2 PZN–0.065PT SC /polyethylene composite at volume fractions of SC $m = 0.1$ (a), $m = 0.2$ (b), $m = 0.3$ (c), and $m = 0.5$ (d)

the $L_{3j}{}^{*}$ factor from Eq. (8) on the orientation dependence of $F_{3j}{}^{*\sigma}$. Of specific interest are equalities of FOMs $(Q_{31}{}^{*})^2 = (Q_{32}{}^{*})^2$ (see Fig. 4) and $F_{31}{}^{*\sigma} = F_{32}{}^{*\sigma}$ (see Fig. 5), which are valid at rotation angles φ near 45°. In this φ region, transverse FOMs $(Q_{31}{}^{*})^2$ and $(Q_{32}{}^{*})^2$ or $F_{31}{}^{*\sigma}$ and $F_{32}{}^{*\sigma}$ are relatively small in comparison to the longitudinal FOM $(Q_{33}{}^{*})^2$ or $F_{33}{}^{*\sigma}$, respectively. Such orientation behaviour of FOMs enables us to state that an appreciable anisotropy of FOMs is achieved at $\varphi \approx 45°–50°$.

A behaviour of longitudinal FOMs $(Q_{33}{}^{*})^2$ and $F_{33}{}^{*\sigma}$ near their absolute maxima is shown in Fig. 6. It is seen that changes in the volume fraction m at the rotation angle $\varphi =$ const lead to more appreciable changes of both $(Q_{33}{}^{*})^2$ and $F_{33}{}^{*\sigma}$. This is achieved due to the strong influence of the dielectric permittivity $\varepsilon_{33}{}^{*\sigma}$ on FOMs $(Q_{33}{}^{*})^2$ and $F_{33}{}^{*\sigma}$, see Eqs. (5)–(7). At small volume fractions $m << 1$, relatively small values of $\varepsilon_{33}{}^{*\sigma}$ are achieved in comparison to the dielectric permittivity $\varepsilon_{33}^{\sigma}$ of the SC component. The orientation dependence of the piezoelectric properties and FOMs at $m =$ const does not contain sharp extreme points [4].

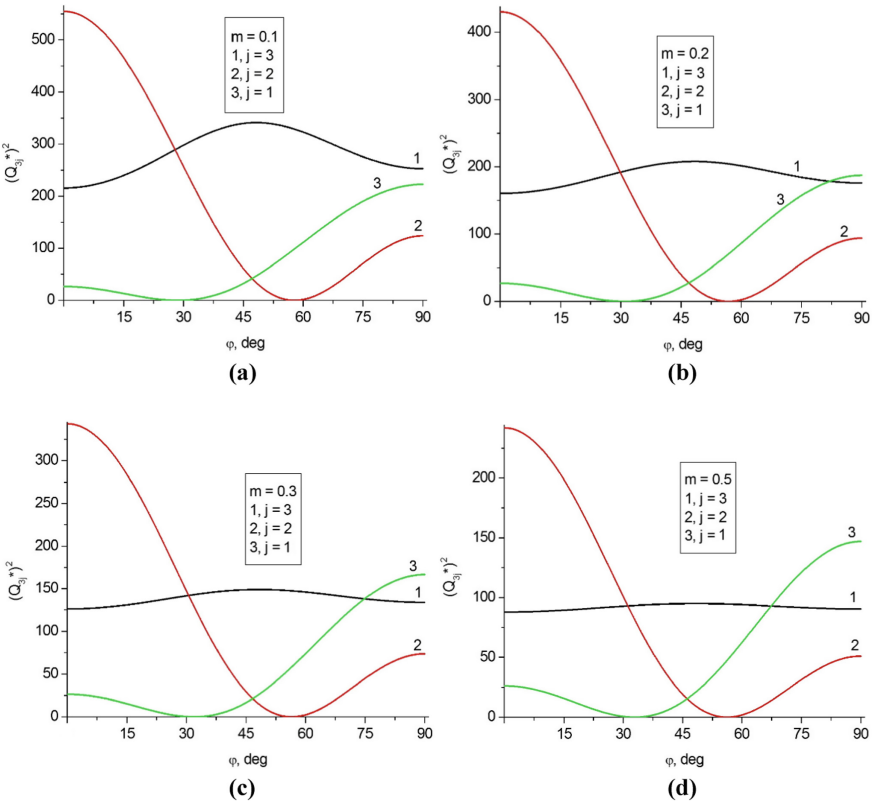

Fig. 4 Orientation dependences of FOMs $(Q_{3j}{}^{*})^2$ (in 10^{-12} Pa^{-1}) of the 2–2 PZN–0.065PT SC /polyethylene composite at volume fractions of SC $m = 0.1$ (a), $m = 0.2$ (b), $m = 0.3$ (c), and $m = 0.5$ (d)

4 Comparison and Discussion

The 2–2 composite, studied in the present chapter, has some advantages over many piezo-active composites known from literature. For example, max $[(Q_{33}{}^{*})^2]$ and max $F_{33}{}^{*\sigma}$ of the 2–2 composite at $m = 0.1$ (see curve 1 in Figs. 4, a and 5, a) are larger than $(Q_{33}{}^{*})^2$ and $F_{3j}{}^{*\sigma}$ of a 1–3 PMN–0.33PT SC / polyurethane composite [11] at the volume fraction of SC $m = 0.05$–0.15. As follows from experimental studies [12], the [001]-poled domain-engineered PMN–0.33PT SC is characterised by the piezoelectric coefficient $d_{33} = 2820$ pC/N. This d_{33} value is about 1.7 times larger than $d_{33} = 1571$ pC/N of the [011]-poled PZN–0.065PT SC (see Table 1). A lead-free 1–3 composite based on the [001]-poled domain-engineered SC is characterised by FOM $(Q_{33}{}^{*})^2 = 23.7 \times 10^{-12}$ Pa^{-1} at the volume fraction of $m \approx 0.52$ [13].

The [011]-poled PZN–0.065PT SC in the main crystallographic axes is characterised by FOMs $(Q_{33})^2 = [Q_{33}{}^{*}(1, 0°)]^2 = 49.8 \times 10^{-12}$ Pa^{-1} and $F_{33}{}^{\sigma} = F_{33}{}^{*\sigma}(1, 0°) = 24.2 \times 10^{-12}$ Pa^{-1}. These constants are evaluated by taking into account experimental data from Table 1. As seen from Fig. 6, absolute maxima of FOMs of the composite are about

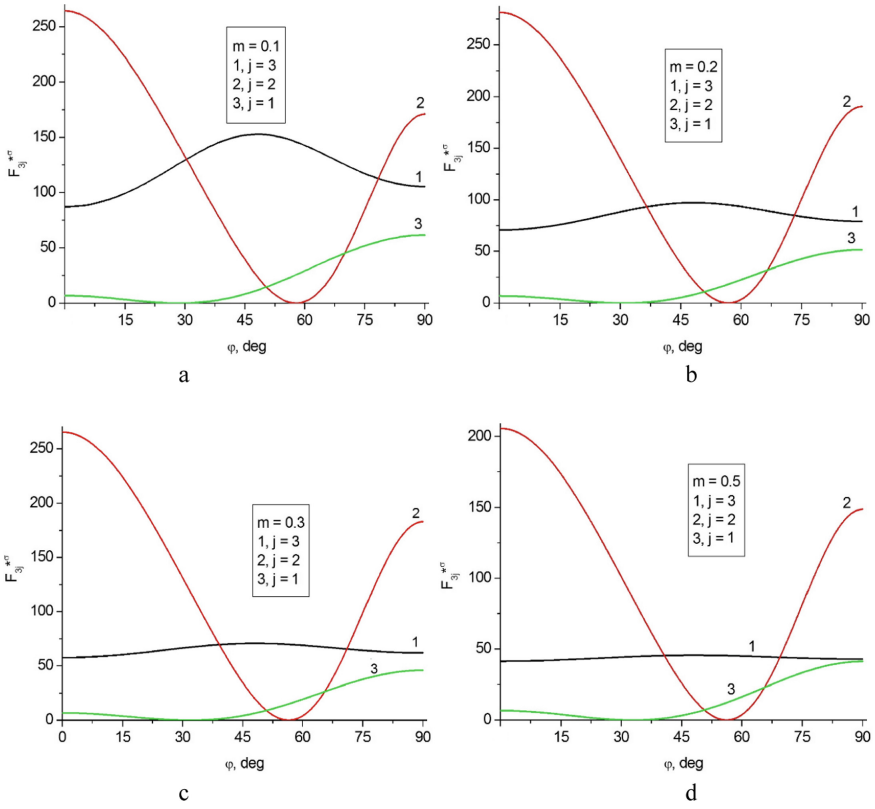

Fig. 5 Orientation dependences of FOMs $F_{3j}{}^{*\sigma}$ (in 10^{-12} Pa^{-1}) of the 2–2 PZN–0.065PT SC / polyethylene composite at volume fractions of SC $m = 0.1$ (a), $m = 0.2$ (b), $m = 0.3$ (c), and $m = 0.5$ (d)

12 times [for $(Q_{33}{}^{*})^2$] or about 9.2 times (for $F_{33}{}^{*\sigma}$) larger than the aforementioned FOMs $(Q_{33})^2$ and $F_{33}{}^{\sigma}$ of the PZN–0.065PT SC at $\varphi = 0°$. Increasing the volume fraction m to 0.1 enables one to obtain longitudinal FOMs $(Q_{33}{}^{*})^2$ and $F_{33}{}^{*\sigma}$ which are approximately five times larger [4] than the similar FOMs of the PZN–0.065PT SC. Such large values of $(Q_{33}{}^{*})^2$ and $F_{33}{}^{*\sigma}$ are obtained even at deviations from the optimal rotation angle by a few degrees [4].

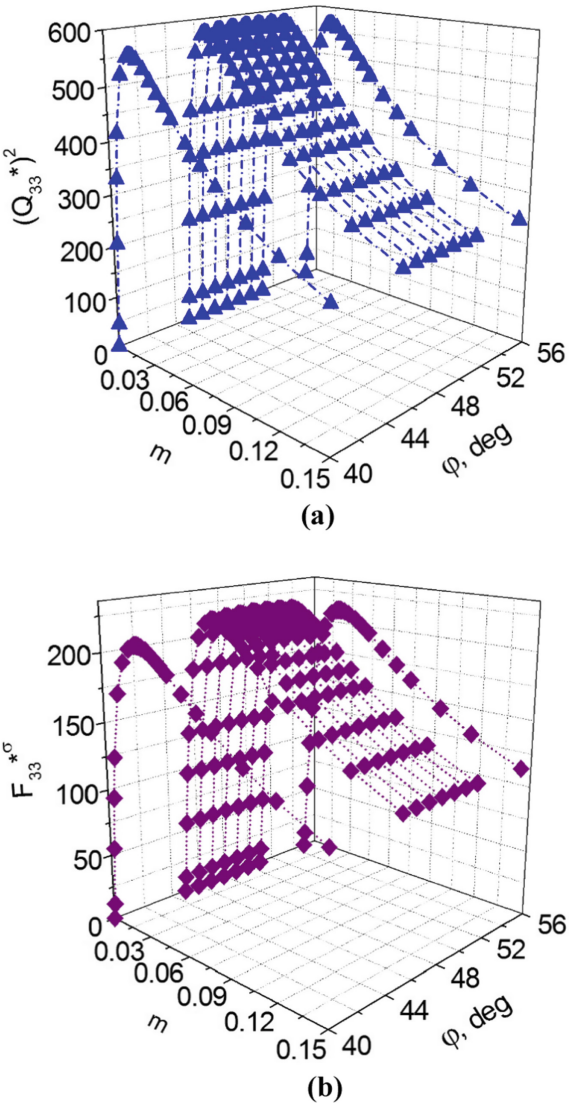

Fig. 6 FOMs $(Q_{33}{}^*)^2$ (a, in 10^{-12} Pa^{-1}) and $F_{3j}{}^{*\sigma}$ (b, in 10^{-12} Pa^{-1}) of the 2–2 PZN–0.065PT SC / polyethylene composite in the vicinity of absolute maximum points (reprinted from paper by Topolov [4], with permission from the Royal Society of Chemistry)

5 Conclusion

The orientation effect concerned with the rotation of the main crystallographic axes X and Y around Z in the SC component (see inset 1 in Fig. 1) has been studied in the 2–2 parallel-connected composite based on the [011]-poled domain-engineered relaxor-ferroelectric PZN–0.065PT SC. The effective piezoelectric properties, ECFs and energy-harvesting FOMs of the composite depend not only on the volume fraction of SC m,

but also on the rotation angle φ. The combination of the SC component, exhibiting the high piezoelectric activity, and the piezo-passive polymer component, exhibiting the large elastic compliance and small dielectric permittivity, would be effective to achieve large values of FOMs $(Q_{3j}{}^*)^2$ and $F_{3j}{}^{*\sigma}$, especially $(Q_{33}{}^*)^2$ and $F_{33}{}^{*\sigma}$ at the longitudinal piezoelectric effect. Changes in the rotation angle φ enable one to reach extremum points of the piezoelectric coefficients $d_{3j}{}^*$ (Fig. 2), ECFs $k_{3j}{}^*$ (Fig. 3), and FOMs $(Q_{3j}{}^*)^2$ (Fig. 4) and $F_{3j}{}^{*\sigma}$ (Fig. 5) at the volume fraction $m = \text{const}$. The similar character of the orientation dependences of the piezoelectric coefficients $d_{3j}{}^*$ and ECFs $k_{3j}{}^*$ (cf. Figs. 2 and 3) is caused by the key role of the proportionality $k_{3j}{}^* \sim d_{3j}{}^*$ from Eq. (4). The similar character of the orientation dependences of FOMs $(Q_{3j}{}^*)^2$ and $F_{3j}{}^{*\sigma}$ (cf. Figs. 4 and 5) is accounted for by a weak influence of the rotation angle φ on the L_{3j}^* factor from Eq. (6).

Taking into account the large piezoelectric coefficients $d_{3j}{}^*$, ECFs $k_{3j}{}^*$, and FOMs $(Q_{3j}{}^*)^2$ and $F_{3j}{}^{*\sigma}$ (see Figs. 2, 3, 4, 5 and 6) of the 2–2 composites and the important orientation effect in them, one can state that these advanced materials are suitable for modern piezoelectric transducers, sensors and energy-harvesting systems.

Acknowledgement. The authors would like to thank Prof. Dr. A. E. Panich and Prof. Dr. I. A. Parinov (Southern Federal University, Russia), Prof. Dr. C. R. Bowen (University of Bath, UK), and Prof. Dr. P. Bisegna (University of Rome Tor Vergata, Italy) for their research interest in the performance of advanced piezo-active composites. Research was financially supported by Southern Federal University, grant No. VnGr-07/2020–04-IM (Ministry of Science and Higher Education of the Russian Federation).

References

1. A. V. Krivoruchko, V. Yu. Topolov. *J. Phys. D: Appl. Phys.* **40**, 7113 (2007).
2. L. Li, S. Zhang, Z. Xu, X. Geng, F. Wen, J. Luo, T. R. Shrout. *Appl. Phys. Lett.* **104**, 032909 (2014).
3. V. Yu. Topolov, P. Bisegna, C. R. Bowen. *Piezo-active Composites. Orientation Effects and Anisotropy Factors*, Springer, Berlin, Heidelberg, (2014).
4. V. Yu. Topolov, C. R. Bowen, A. V. Krivoruchko, A. N. Isaeva. *CrystEngComm* **24**, 1177 (2022).
5. R. Zhang, B. Jiang, W. Jiang, W. Cao. *Appl. Phys. Lett.* **89**, 242908 (2006).
6. C. He, W. Jing, F. Wang, K. Zhu, J. Qiu. *IEEE Trans. Ultrason., Ferroelec., a. Freq. Contr.* **58**, 1127 (2011).
7. S. Zhang, L. C. Lim. *AIP Advances.* **8**, 115010 (2018).
8. J. I. Roscow, H. Pearce, H. Khanbareh, S. Kar-Narayan, C. R. Bowen. *Eur. Phys. J.: Spec. Top.* **228**, 1537 (2019).
9. A. N. Isaeva, V. Yu. Topolov, C. R. Bowen, J. I. Roscow. *Mater. Chem. Phys.* **279**, 125691 (2022).
10. C. R. Bowen, V. Yu. Topolov, H. A. Kim, *Modern Piezoelectric Energy-harvesting Materials*, Springer International, Cham, (2016).
11. V. Yu. Topolov, A. N. Isaeva. *Tech. Phys.* **66**, 938 (2021).
12. R. Zhang, B. Jiang, W. Cao. *J. Appl. Phys.* **90**, 3471 (2001).
13. D. Zhou, K. H. Lam, Y. Chen, Q. Zhang, Y. C. Chiu, H. Luo, J. Dai, H. L. W. Chan. *Sens. a. Actuators A.* **182**, 95 (2012).